Journal of Thermal Analysis and Calorimetry (2024) 149:5047–5057
https://doi.org/10.1007/s10973-024-12994-z

Impact of hybrid nanofluid on thermal behavior of flat-plate solar collector: performance study

Lokesh Selvam[1] · M. Aruna[2] · Ismail Hossain[3] · R. Venkatesh[4] · M. Karthigairajan[5] · S. Prabagaran[6] · V. Mohanavel[7,8] · A. H. Seikh[9] · Md. Abul Kalam[10]

Received: 5 November 2023 / Accepted: 14 February 2024 / Published online: 12 March 2024

Abstract

Energy consumption in buildings is a major contributor to India's greenhouse gas emissions, accounting for a significant portion of the country's environmental impact. Consequently, there is a crucial need to prioritize energy-efficient heating, ventilation, and air conditioning technologies supported by solar thermal collectors to minimize the environmental consequences associated with building energy consumption. In this investigation, a flat-plate collector thermal performance is enhanced by the adaptations of 0.1 volume percentage concentrations of aluminum oxide (Al_2O_3), nickel (Ni), and combinations of Al_2O_3–Ni nanoparticles dispersed in water as hybrid nanofluid at 0.028, 0.041, 0.055, and 0.068 kgs^{-1} flow rates. Influences of nanofluid and flow rate conditions on thermal and exergy efficiency, heat transfer coefficient, entropy generation, and coefficient of performance of FPC are experimentally analyzed and spot that the hybrid nanofluid (Al_2O_3/Ni/water) own higher thermal and exergy efficiency of 72.8% and 22.9%, better heat transfer coefficient of 133.2 $Wm^{-2}\,K^{-1}$, and high COP of 7.9 under high flow rate. These output results are higher than those of the water-fluid-operated FPC.

Keywords Flat-plate collector · Heating, ventilation, and air conditioning · Nanofluid · Thermal performance: coefficient of performance

Abbreviations

A_c	Collector area (m^2)
Al_2O_3	Aluminum oxide
C_p	Specific heat of fluid ($J\,kg^{-1}\,K^{-1}$)
COP	Coefficient of performance
D	Tube diameter (m)
F_R	Heat removal factor
Fe_2O_4	Iron dioxide
FPC	Flat-plate collector
H	Heat transfer coefficient ($Wm^{-2}\,K^{-1}$)
HVAC	Heating, ventilation, and air conditioning
I	Solar radiation (Wm^{-2})
K	Thermal conductivity ($Wm^{-1}\,K^{-1}$)
$\dot{m}$	Flow rate of fluid (kgs^{-1})
MgO	Magnesium oxide
MWCNT	Multi-walled carbon nanotubes
Ni	Nickel
Nu	Nusselt number

✉ R. Venkatesh
venkidsec@gmail.com

[1] Department of Mechanical Engineering, SRM Institute of Science and Technology, Ramapuram Campus, Chennai 600 089, Tamil Nadu, India

[2] Department of Industrial Management, Faculty of Business, Liwa College, Abu Dhabi, UAE

[3] Department of Nuclear and Renewable Energy, Ural Federal University, Yekaterinburg 620002, Russia

[4] Department of Mechanical Engineering, Saveetha School of Engineering, Saveetha Institute of Medical and Technical Sciences (SIMATS), Saveetha University, Chennai 602105, Tamil Nadu, India

[5] Department of Mechanical Engineering, Karpaga Vinayaga College of Engineering and Technology, Chengalpattu 603308, Tamil Nadu, India

[6] Department of Mechanical Engineering, Karpagam Academy of Higher Education, Coimbatore 641021, Tamil Nadu, India

[7] Centre for Materials Engineering and Regenerative Medicine, Bharath Institute of Higher Education and Research, Chennai 600073, Tamil Nadu, India

[8] Department of Mechanical Engineering, Amity University, Dubai 345019, United Arab Emirates

[9] Mechanical Engineering Department, College of Engineering, King Saud University, 11421 Riyadh, Saudi Arabia

[10] School of Civil and Environmental Engineering, FEIT, University of Technology, Sydney, Ultimo, NSW, Australia

Q_u	Heat gain (W)
Q_{in}	Energy input (W)
S	Entropy generation (W K^{-1})
SiO_2	Silicon dioxide
T_{amb}	Ambient temperature (K)
T_{in}	Inlet temperature (K)
T_{out}	Outlet temperature (K)
T_{sun}	Sun temperature (5770 K)
U_l	Heat loss coefficient (Wm^{-2} K^{-1})

Greek symbol

τ	Transmittance
α	Absorptivity
η_{th}	Thermal efficiency (%)
η_e	Exergy efficiency (%)

Introduction

The HVAC systems are integral to modern living, offering comfort and climate control. Their projections indicate that this energy demand could surge by a factor of 4.3 by 2037. Such a dramatic increase in energy consumption due to HVAC systems could significantly worsen environmental pollution [1]. Hence, the primary sources of electricity generation worldwide depend on fossil fuels like natural gas, oil fuel, and coal. Solar energy is a fast-growing and popular renewable source retained with collectors' help, with flat plates, evacuated tubes, dish collectors, and parabolic troughs for HVAC applications. Specifically, flat-plate solar collectors (FPC) are uncomplicated and capable of operating efficiently within a temperature range of up to 150 °C. Hence, the FPC is a viable and effective option for integrating HVAC systems [2]. The choice of working fluid for solar systems plays a pivotal role in determining the efficiency of FPC. To enhance the thermal performance of FPC, numerous researchers have conducted studies utilizing various working fluids, such as water, oil, and nanofluids (base fluids with dispersed nanoparticles). Incorporating nanofluids within solar collectors notably impacts collector performance by improving the working fluid thermal characteristics [3].

FPC with a hybrid nanofluid at a concentration of 0.15% significantly enhances heat transfer and exhibits a remarkable peak Nusselt number enhancement of approximately 21.2% [4]. When integrated with FPC, the MgO/water nanofluid outperformed the Al_2O_3/water nanofluid in terms of thermal performance improvement, demonstrating its superior capabilities [5]. The Al mixed with alumina/water combinations of hybrid nanofluid is considered a working medium, exhibiting a superior performance improvement of about 23.6% [6]. Utilizing the Ni/Fe_2O_4 nanofluid at higher flow rates significantly enhances the effectiveness of the FPC, resulting in an impressive efficiency of 22% compared to traditional water [7]. Employing Al_2O_3–SiO_2/water hybrid nanofluid at 0.5%, 1%, and 1.5% concentration resulted in a remarkable increase of 25%, 60%, and 67% in HTC [8]. Utilizing a hybrid MWCNT/Al_2O_3 (50:50) combination leads to efficiency improvements of 26%, 29%, and 18% at flow rates of 1.5, 2.5, and 3.3 LPM, respectively. It suggests that substituting 50% of the more expensive MWCNTs with environmentally friendly Al_2O_3 is a viable recommendation [9]. Experiments with different Al_2O_3 concentrations ranging from 1 to 4% in FPC showed that the 4% concentration yielded the highest thermal efficiency, reaching approximately 67.1%, surpassing the efficiencies achieved with other concentration levels [10].

Moreover, the choice of working fluid significantly impacts the COP within the HVAC system. The highest COP value, approximately 0.86, was achieved when utilizing alumina/water nanofluid [11]. The nanofluid-based system was recently reviewed, summarizing the thermal performance for automotive cooling applications. Compared to water-fluid-operated radiators, nanofluids recorded better thermal conductivity [12]. Besides, the adaptations of multi-walled carbon nanotube-based terminal 55 nanofluid with varied volume percentages noted better thermal conductivity [13]. The thermal performance of solar collectors is improved by using modified fin, nanofluid, and coating material [14]. Based on this, recent research is exposed with copper oxide (CuO) nanoparticles and matt black paint coated with an absorber unit implemented as single slope solar. Its thermal performance is experimentally evaluated. Its output showed a 19.90% improved exergy compared to the conventional solar system [15].

Moreover, nanofluid technology with a suitable solar collector design found better thermal behavior and improved thermal conductivity [16, 17]. Solar-based thermal energy utilization for concentrating solar power in environmental aspects is discussed [18]. The solar collector efficiency is enriched by introducing magnesium oxide and multi-walled nanotube hybrid nanofluid in 80–20, 70–30, 60–40, and 50–50 ratios under 1–3 L min^{-1} flow rate. They reported that the hybrid nanofluid 50–50 ratio performed maximum energy and exergy efficiency of the collector [19]. Likewise, much research has been carried out related to nanofluids such as alumina, copper oxide, and iron oxide [20–22]. However, the solar performance varies due to weather conditions and time [23]. The literature review has revealed that existing research on nanofluids for enhancing heat transfer in FPC systems is limited and primarily focused on specific types of nanofluids. These studies have shown favorable results when replacing the combinations of water mixed with nanoparticles (nanofluid) considered the working fluid, leading to increased thermal conductivity and HTC and improved system efficiency. However, it is noteworthy

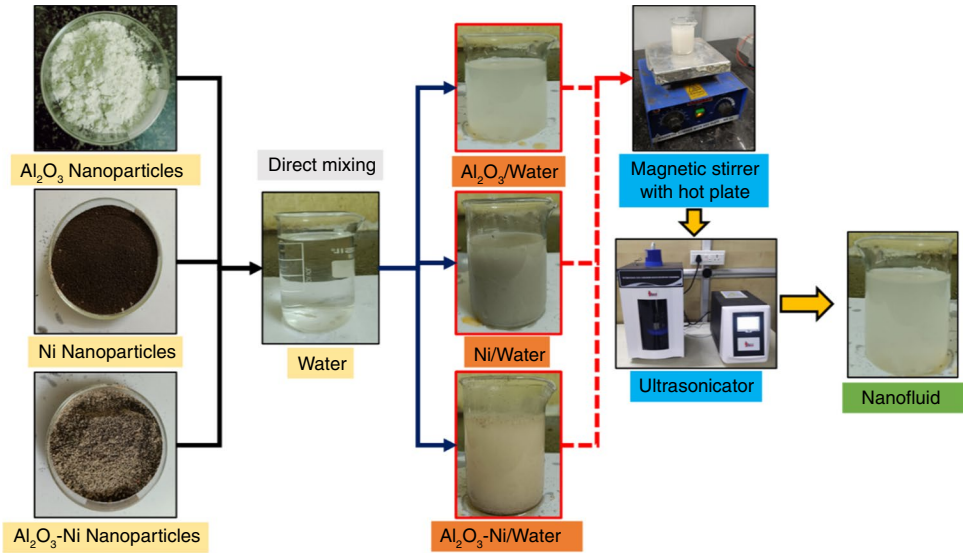

Fig. 1 Photocopy of nanofluid preparation

that these studies have employed various methodologies and produced varying findings. Furthermore, it is advisable to explore the potential of different types of nanoparticles in nanofluid preparation when integrated with FPC systems for HVAC applications. However, the literature on integrating Al_2O_3, Ni, and Al_2O_3/Ni nanofluids with the HVAC system using FPC's was unavailable.

This study delves into the thermal performance evaluation of FPC designed for HVAC applications. The investigation encompasses diverse working fluid conditions, incorporating water and nanofluids, such as Al_2O_3, Ni, and Al_2O_3/Ni, at a 0.1% volume fraction when dispersed in water. A specific ratio of 50:5 between water and nanofluid was selected. Introducing nanofluids into the FPC system notably impacts its thermal characteristics, progressively enhancing the working fluid's thermal properties. Specifically, Al_2O_3/Ni nanofluid exhibits superior performance across various aspects, including thermal and exergy efficiency, HTC, Nusselt number, and entropy generation. Furthermore, this nanofluid optimizes the COP within the cooling circuit of the HVAC system, signifying its potential to enhance overall system efficiency.

Material and method

Preparation of nanofluids

Here, combinations of water and nanofluid, which contain Al_2O_3, Ni, and Al_2O_3–Ni, each with a diameter ranging from 40 to 60 nm, are to be used. As mentioned earlier, the varied particle size exploited superior thermal conductivity [12]. They were employed as the working fluids in the FPC heat pipe. They were tested under different flow rate conditions of 0.028, 0.041, 0.055, 0.068, and 0.083 kgs^{-1}, respectively. These nanoparticles were chosen based on their high thermal conductivity, chemical inertness as a base fluid, and cost-effectiveness rather than others [24, 25]. The specific reason for selecting metal oxide particles is their unique thermal properties and cost-effectiveness compared to others [12]. As earlier [9], the thermal performance of FPC is evaluated with a hybrid nanofluid with 0.005–0.01 vol% concentration, and more than 0.01 vol% showed better results. Likewise, 0.1% of the Al_2O_3 blend attained maximum thermal efficiency [11]. This study is fixed as these nanoparticles' 0.1% volume fraction concentration was blended with the working fluid and thoroughly stirred. In the case of Al_2O_3–Ni, a mixture of 50% of each component was used, and its nanofluid preparation is exposed in Fig. 1. A magnetic stirrer was consistently utilized to ensure the creation of a uniform suspension, and the hot plate was raised to 300 °C. To enhance the nanofluid stability, the water–Al_2O_3, water–Ni, and water–Al_2O_3–Ni hybrid nanofluids are involved in the ultrasonication process at higher sonication duration [13].

As mentioned earlier [26], different water-based nanofluids prepared with a four-day sonication process exposed better stability for up to 33 days, and more than four days showed the micrometric aggregate results of partial instability. With this concern, the present Al_2O_3–Ni nanofluid is prepared with continuous pulsing through an ultrasonication device for four days to achieve the desired stability from the first to 32 days (constant) and homogeneity. The dynamic light scattering (DLS)-analyzed stability values are highlighted in Table 1. The water and nanofluid properties, [5] and [25], are in Table 2.

Table 1 DLS analyzed the mean diameter of nanoparticles (static sample)

Nanoparticles	Preparation days	Concentration	Method	Peaks (mean diameter—50 nm)
Ni	4	0.1 vol%	Ultrasonication	193
Al_2O_3	4			178

Table 2 Properties of working fluid

Working fluid	Density/kg m^{-3}	Heat capacity/Jkg^{-1} K^{-1}	Thermal conductivity/Wm^{-1} K^{-1}
Water	997.6	4184	0.6
Al_2O_3	3600	451	35
Ni	8900	445	106

Experimental

Saveetha University's geographical location of the present investigation is in Chennai, the capital city of the Indian state of Tamil Nadu. Its geographical coordinates are approximately 13.0604°N latitude and 80.1831°E longitude. The incident average (annual) global horizontal irradiance for Saveetha University in Chennai is typically from 5.5 to 6.0 kWh m^{-2} per day. In this experiment, the FPC was inclined at an angle of 30 degrees due to optimum sunlight absorption. Two working fluids, namely water and nanofluid, were circulated through the system at varying flow rates. The working fluid flow rate was monitored using a flow meter and controlled using a valve. The fluid inlet and outlet temperatures were monitored and recorded using J-type thermocouples connected in a series to a data logging system. The heat from hot fluid was efficiently transferred to the HVAC circuit through a heat exchanger. Simultaneously, ambient temperature data were recorded to facilitate the calculation of relevant thermal parameters. Solar radiation levels were also measured using a pyranometer and an advanced anemometer to determine wind speed. It is important to note that all system components were designed to provide complete isolation, ensuring that heat transfer occurred exclusively between the working fluids. For this study, the water and nanofluid were taken as 50:5. With the conditions of a quasi-steady state, the values are noted to maintain integrity and accuracy. Figure 2 shows the experimentation layout for the current study.

Instantaneous efficiency values were determined by the combinations of inlet fluid temperature, incident radiation, and ambient temperature, enabling the FPC's thermal performance calculation. Under various flow rate conditions, the experimental work spanned five consecutive days between 10:00 and 15:00 for 30 min intervals.

Graphs were constructed to visualize the experimental results, illustrating how FPC efficiency correlates with the reduced temperature parameter $[(T_{in} - T_{amb})/I]$. The experiments were carried out over multiple days, with the most favorable results chosen for analysis. Throughout the tests, the largest fluctuations in an inlet and ambient temperatures remained within ±0.6 and ±0.8 °C. Furthermore, significant changes in global radiation are observed by ±28 Wm^{-2}. These observations confirm that the experiments were conducted under quasi-steady state conditions in compliance with the ASHRAE policy of 93–2003 [30]. The efficiency of FPC was evaluated by different rates of flows ranging from 0.028 to 0.083 kgs^{-1}, providing a comprehensive assessment of its performance under different flow conditions. Figure 3 shows the photocopy of the experiment and its equipment specification, addressed below in Table 3.

During the experiments, the following assumptions are made. The blending of nanoparticles is homogenous, with uniform solar irradiance, constant nanoparticle concentrations, and negligible heat loss permitted. Likewise, the flow rate varies from 0.028 to 0.068 kgs^{-1}. Moreover, the following assumptions made during the experimental investigations included that the flow is in a steady state, good adsorption behavior with their loss considered as less than 1%, and there was minimum convective and radiation loss (less than 1%). For this reason, higher thermal performance during high flow rates may be shown.

Thermal analysis

The measured value from this section is used to measure the performance of FPC. The heat gain by FPC is measured by the ratio of output and input energy, which is mentioned in Eqs. (1) and (2) [15].

$$Q_u = \dot{m}C_p(T_{out} - T_{in}) \tag{1}$$

$$Q_{in} = AcI \tag{2}$$

The energy of the system related to the approach of absorption and loss is mentioned in Eqs. (3) and (4) [16]:

$$Q_u = A_c F_R[I(\tau\alpha) - U_l(T_{in} - T_{amb})] \tag{3}$$

$$\begin{aligned}\eta_{th} &= \frac{Q_u}{Q_{in}} = \frac{\dot{m}C_p(T_{out} - T_{in})}{A_c I} \\ &= \frac{A_c F_R[I(\tau\alpha) - U_l(T_{in} - T_{amb})]}{A_c I} \\ &= F_R(\tau\alpha) - F_R U_l \frac{T_{in} - T_{amb}}{I}\end{aligned} \tag{4}$$

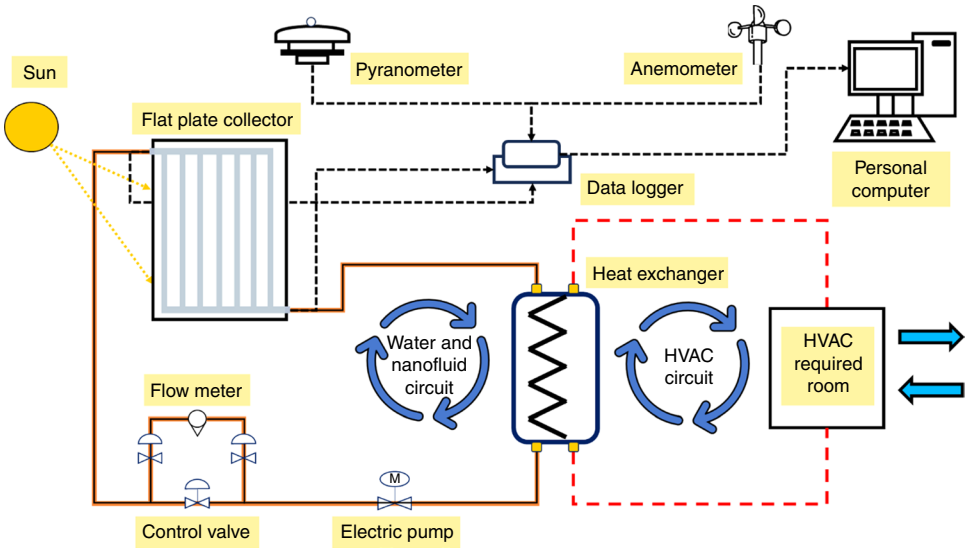

Fig. 2 Systematic layout of FPC experimental setup

In Eq. (5), $\frac{T_{in}-T_{amb}}{I}$, F_R, U_L, τ, and α illustrate the minimized temperature parameters. The Nusselt number by working fluid is defined as

$$Nu = \frac{hD}{k} \tag{5}$$

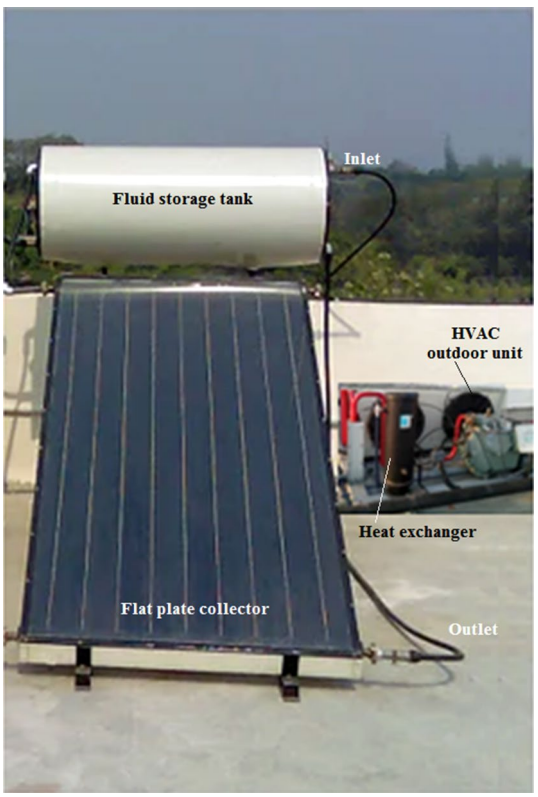

Fig. 3 Actual experimental setup of FPC

Here, h is the HTC, D is the absorber tube diameter, and k is the thermal conductivity. The entropy generation is given by Eq. (6).

$$\Delta S = S_{out} - S_{in} = C_p \ln\left(\frac{T_{out}}{T_{in}}\right) - R\ln\left(\frac{P_{out}}{P_{in}}\right) \tag{6}$$

Following Eqs. (7–11) measure the exergy efficiency.

$$\eta_e = \frac{\dot{E}_{useful}}{\dot{E}_{solar}} \tag{7}$$

$$\dot{E}_{useful} = \dot{E}_{out} - \dot{E}_{in}$$

$$\dot{E}_{out} = \dot{m}C_p\left[\left(T_{out} - T_{amb}\right) - T_{amb}\ln\left(\frac{T_{out}}{T_{amb}}\right)\right] \tag{8}$$

$$\dot{E}_{in} = \dot{m}C_p\left[\left(T_{in} - T_{amb}\right) - T_{amb}\ln\left(\frac{T_{in}}{T_{amb}}\right)\right] \tag{9}$$

Table 3 Specification of the FPC

Area of FPC	2500 mm × 1000 mm
Fluid medium	Water, Al_2O_3, Ni, and Al_2O_3/Ni hybrid nanofluid
Inner dia. of tube	15 mm
Outer dia. of the tube	15.5 mm
Slope	30°
Center distance of the tube	70 mm
Material for the back plate	Aluminum
Collector cover	Toughened glass of 3 mm thickness

Table 4 Measured instrument uncertainty

Name of instrument	Instrument model	Range	Uncertainty
Anemometer	FST200-1000	0.5–50 ms^{-1}	0.02%
Data logger	KEY34970A	− 200–800 °C	±0.5 °C
Pyranometer	SMP11	0-4000W m^{-2}	0.5%
Thermocouple	WRNK-191	0–600 ^{O}C	0.5%

$$\dot{E}_{solar} = AcI\left[1 + \frac{1}{3}\left(\frac{T_{amb}}{T_{sun}}\right) - \frac{4}{3}\left(\frac{T_{amb}}{T_{sun}}\right)\right] \tag{10}$$

$$\mathrm{COP} = \frac{Q_c}{W_{in}} \tag{11}$$

Here, is Q_c heat dissipation by refrigerator, and W_{in} is work input.

Uncertainty analysis

To evaluate the error in calculated thermal performance, an uncertainty analysis is executed for all data gained from experimentation in the present study, which can be expressed as Eq. (12) [17].

$$w_x = \sqrt{\left(\frac{\partial X}{\partial x_1}\right)^2 (wx_1)^2 + \left(\frac{\partial X}{\partial x_2}\right)^2 (wx_2)^2 + \ldots\ldots\cdots + \left(\frac{\partial X}{\partial x_n}\right)^2 (wx_n)^2} \tag{12}$$

where w_x is uncertainty, wx_n is measured value uncertainty, and x_n is an uncertainty variable. Table 4 shows the uncertainty of measured instruments.

Results and discussion

Thermal efficiency

Figure 4a–d depicts how thermal efficiency varies with the $T_{in} - T_{amb}/I$ parameter. The working fluid thermal behaviors are enhanced when nanoparticles are dispersed, leading to differences in FPC efficiency as water temperature parameter decreases for various flow rates and working fluids. Further, the thermal efficiency decreases as the reduced temperature parameter ($T_{in} - T_{amb}/I$) increases at most points. In Fig. 4a, the highest thermal efficiency using water is achieved at 32.5%, 39.4%, 45.1%, and 50.2% for flow rates of 0.028, 0.041, 0.055, and 0.068 kgs^{-1}, respectively. It demonstrates that an increased rate of flow finds superior efficiency. Consequently, the highest flow rate consistently yields superior thermal efficiency compared to other flow rate conditions.

With Al_2O_3 nanofluid, the optimal (peak) efficiency at flow rates of 0.028, 0.041, 0.055, and 0.068 kgs^{-1}, as shown in Fig. 4b, is about 48.6%, 52.7%, 61.5%, and 67.3%. The enhancement of thermal efficiency was the primary reason for the presence of Al_2O_3.

As earlier, Salman et al. [7] studied and reported that the alumina-blended nanofluid facilitates higher thermal efficiency related to water medium. Likewise, Fig. 4c reveals that at the same flow rate conditions, the peak efficiency reaches approximately 54.3%, 62.7%, 69.6%, and 75.3% when using Ni nanofluid. While compared with alumina and water fluid, it offered maximum efficiency due to its enhanced thermal conductivity, as represented in Table 2. Besides, the hybrid combinations of nanofluids were exploited more than the conventional fluid [31]. Furthermore, Fig. 4d illustrates that by using Al_2O_3–Ni nanofluid, the optimal efficiency at flow rates of 0.028, 0.041, 0.055, and 0.068 kgs^{-1} is about 65.9%, 71.6%, 83.2%, and 94.1%, respectively. Thus, Al_2O_3–Ni nanofluid demonstrates superior efficiency compared to other nanofluids and water. In addition, this Al_2O_3–Ni nanofluid combination facilitates higher thermal efficiency rather than the past reported value of 49.7% [24].

Similarly, Fig. 5 shows the average thermal efficiency value for water and nanofluid at dissimilar flow rates. The average efficiency by water is 24.1%, 30.8%, 34.4%, and 38.6%, respectively, at 0.028, 0.041, 0.055, and 0.068 kgs^{-1}. At the same time, average efficiency for Al_2O_3–Ni shows the superior efficiency than water of about 51.7%, 58.6%, 66.9%, and 72.8%. The progression of efficiency with increasing flow rates predominantly stems from enhanced heat transmission properties [18, 19]. Incorporating nanoparticles like Al_2O_3 and Ni further augments efficiency because of their elevated heat transfer and thermal conductivity attributes. Remarkably, Al_2O_3–Ni nanofluid surpasses other alternatives by capitalizing on the advantages of both nanoparticle types, resulting in superior thermal efficiency compared to conventional nanofluids and pure water.

Exergy efficiency

Figure 6 depicts an FPC's average exergy efficiency using water and nanofluids at various flow rates. Notably, using Al_2O_3–Ni nanofluid as the working fluid in FPC for HVAC systems significantly impacts exergy efficiency. These hybrid nanofluids establish it as a more effective absorbing medium than water. At the same time, at 0.028 kgs^{-1} flow rate, the exergy efficiency of the system to be achieved with water, Al_2O_3, Ni, and Al_2O_3–Ni is 7.5%, 8.7%, 9.5%, and 11.6%, respectively. Likewise, the 0.068 kgs^{-1} flow rate reaches a better exergy efficiency of 13.4%, 15.9%, 20.3%, and 22.9% for the same working fluid conditions. This hybrid nanofluid operated with a higher flow rate and showed a 22.9% exergy efficiency, higher than the water fluid.

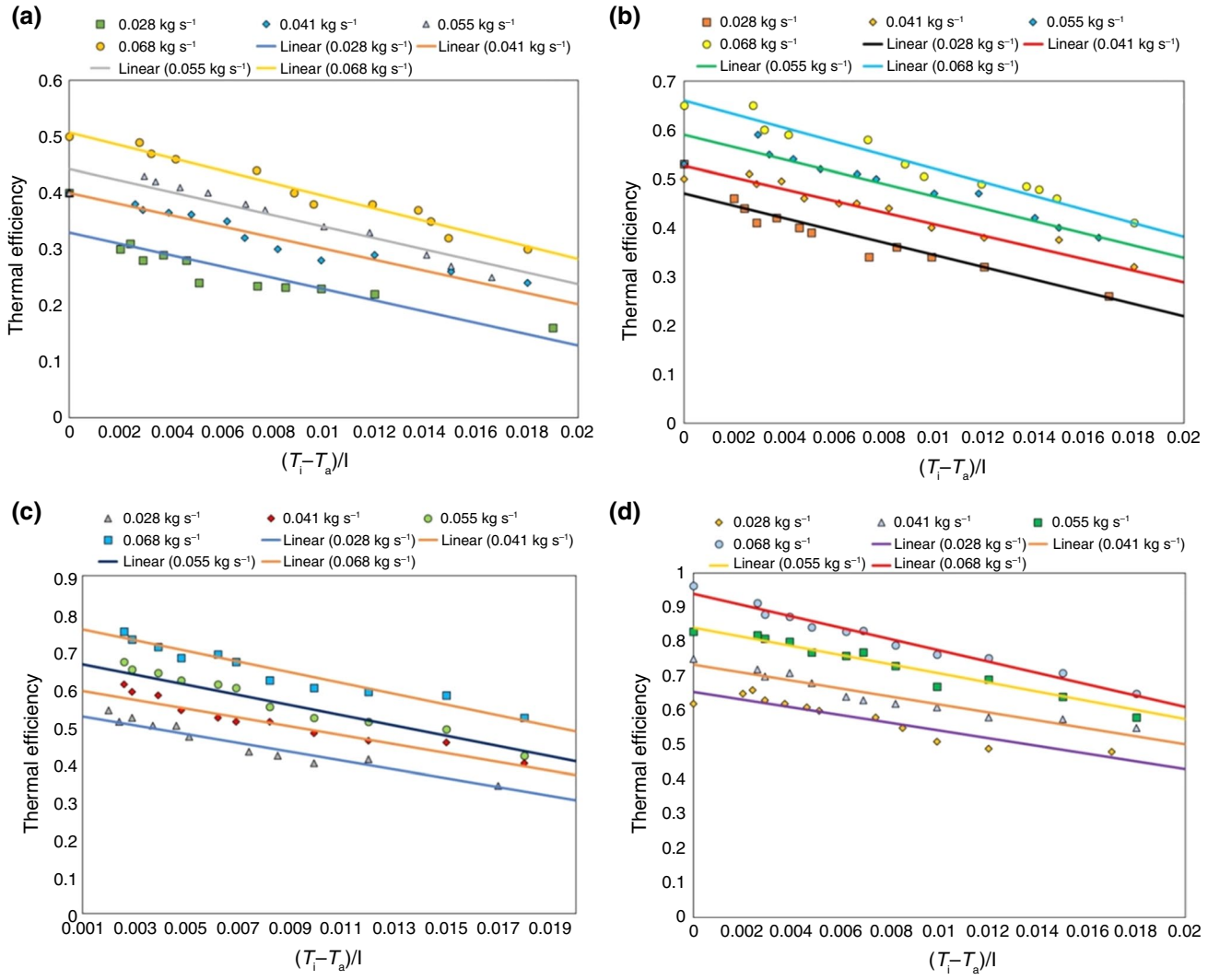

Fig. 4 Thermal efficiency vs. temperature difference parameter **a** water, **b** Al_2O_3, **c** Ni, and **d** Al_2O_3–Ni

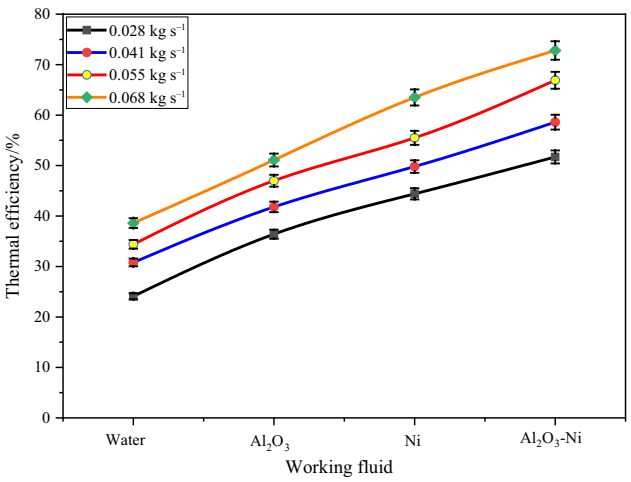

Fig. 5 Average thermal efficiency for different flow rates

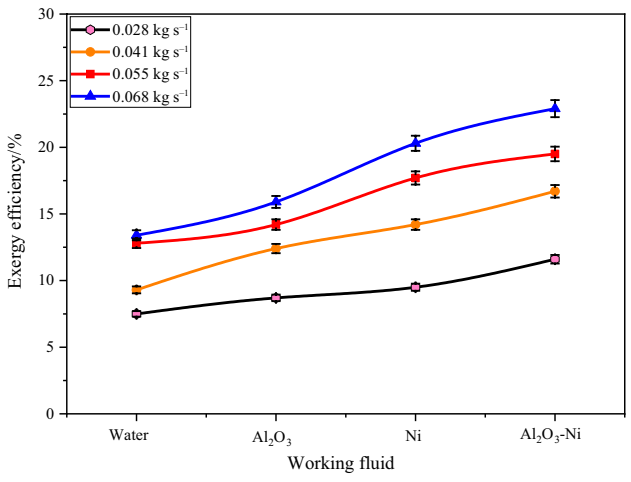

Fig. 6 Average exergy efficiency for different flow rates

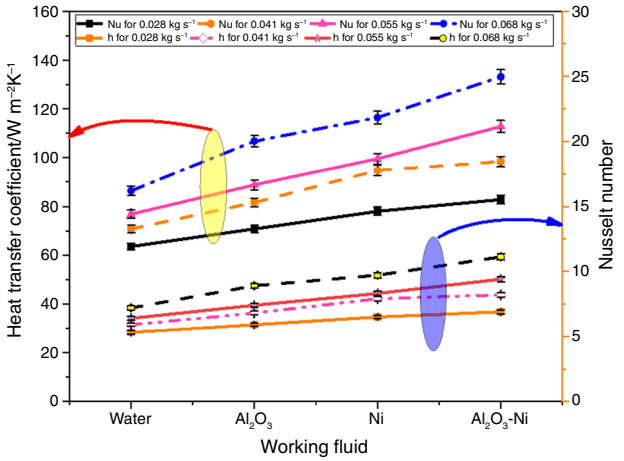

Fig. 7 Average HTC and Nusselt numbers for different working conditions

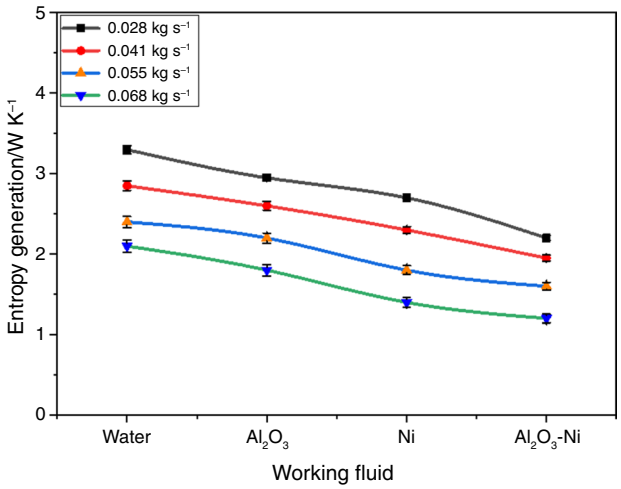

Fig. 8 Entropy generation for working fluid

Moreover, the exergy efficiency is higher than the water fluid. It may vary due to the flow rate of nanofluid and its concentration. As mentioned earlier, the hybrid nanofluid (Al_2O_3/MWCNT) was found to have 34% exergy efficiency under 0.058 kgs^{-1} [9]. Here, less than 5% pressure drop is considered due to the utilization of different nanofluid at varied flow rates, and the lack of efficiency may be caused by the mismatch of thermal conductivity and compatibility of material [11].

During the evaluation, the nanofluid and its flow rate varied with a similar FPC setup, leading to a pressure drop and being considered less than 5%. It is one reason for limited exergy efficiency compared to Al_2O_3 and Ni nanofluid-functioned FPC. The synergistic influence of these nanoparticles within Al_2O_3–Ni nanofluid significantly enhances its heat transfer capabilities, resulting in a distinct advantage in exergy efficiency related to other nanofluids. It underscores the promise of nanofluids, specifically focusing on Al_2O_3–Ni nanofluid, for optimizing the performance of HVAC systems employing FPC. The utilization of Al_2O_3/water nanofluid significantly enhances exergy efficiency, with an impressive increase of up to 21%.

HTC and Nusselt number

Both the HTC and Nusselt numbers are crucial in determining the thermal performance of FPC's. The increase in temperature gradient causes variations in the Nusselt number, as these factors influence the HTC. Further, increasing the flow rate could enhance the HTC Nusselt number and improve FPC performance, connected with boundary conditions of fluid's heat transfer under the convection forced flow.

Figure 7 illustrates HTC and Nusselt number variation for varied rates of flow. Here, the 0.068 kgs^{-1} flow rate and the HTC and Nusselt numbers for water are approximately 86.4 Wm^{-2} K^{-1} and 7.2, respectively. In contrast, when using Al_2O_3–Ni nanofluid, the average HTC and Nusselt numbers are elevated to around 133.2 W m^{-2} K^{-1} and 11.1. The nanofluid significantly enhances heat transfer efficiency, resulting in higher HTC and Nusselt number values than water as the working fluid. Specifically, the alumina nanofluid rather than water enhances the HTC and Nusselt numbers by about 19.5% and 58%, respectively. It also increases their behavior-wise HTC, thermal behavior, and heat transfer rate [21].

Entropy generation and COP

The amount of entropy generated by the FPC plays a crucial role in determining the FPC's energetic performance. It is a critical factor that must be managed to ensure maximum FPC efficiency. The concentration of nanoparticles is kept constant, and the value of entropy generation was obtained at different working fluids at various flow rate conditions, as shown in Fig. 8.

Increasing the nanofluid flow rate decreases the entropy generation rate, which is inversely proportional to the exergy efficiency of the collector. Here, the entropy generation of water and nanofluid system is shown as a downtrend. Here, the entropy generation of water fluid is 3.3, 2.85, 2.4, and 2.1 W K^{-1} at an increased flow rate from 0.028 to 0.068 kgs^{-1}. Likewise, the nanofluid and hybrid nanofluid found decreased entropy generation due to irreversible thermal performance action, which improved exergy efficiency.

Similarly, the coefficient of performance (COP) for the cooling unit within the HVAC circuit during the FPC experimentations using nanofluid was computed. Figure 9 illustrates the variations in COP for the HVAC cooling unit with different working fluids. Notably, with a 0.028 kgs^{-1}

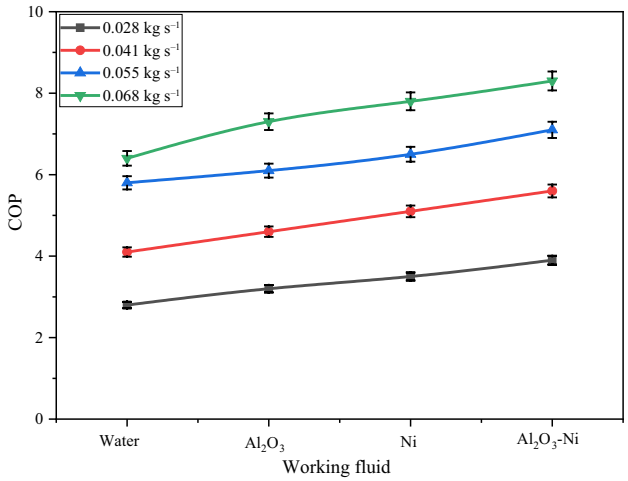

Fig. 9 COP of the cooling system using various working fluids

flow rate, COP is approximately 2.8, 3.2, 3.5, and 3.9 for water, Al_2O_3, Ni, and Al_2O_3–Ni, respectively. Similarly, under the same working fluid conditions, with an optimal flow rate of 0.068 kgs^{-1}, the COP reaches around 6.4, 7.3, 7.8, and 8.3. Therefore, nanofluids, especially at higher flow rates, consistently exhibit higher COP values than water. The results indicate that using nanofluids, especially Al_2O_3–Ni nanofluid, and operating at higher flow rates can significantly enhance the COP of the HVAC cooling unit. This improvement in COP is essential for achieving better cooling efficiency and maintaining a comfortable indoor environment in HVAC systems [23]. Table 5 compares the thermal performance of FPC using various nanofluids to the current study's findings.

According to Table 5, the present FPC adopted with 0.1% concentrations of Al_2O_3/water, Ni/water nanofluid, and water: Al_2O_3/Ni with ratios of 50:5 nanofluid operated with 0.068 kgs^{-1} flow rate FPC found better thermal efficiency compared to the recent literature. In this FPC, thermal efficiency improved by 72.8%, which is higher than the reported values of Tong et al. [20] and Azim et al. [25] (56.9 and 44.96%).

Economic and environmental impact summary

Here, we summarized the work feasibility related to the economic and environmental impact of the present research. The nanofluid-adopted FPC showed better thermal performance, such as improved temperature, thermal efficiency, exergy efficiency, HTC, entropy, and COP, compared to copper oxide-based nanofluid. The Al_2O_3 and Ni-based nanofluid is cost-effective with improved energy savings. The details of energy saving and its environmental conditions are addressed in Table 6.

The thermal and exergy energy savings are calculated using the water-operated FPC system. The thermal energy is saved by 33.9, 73.31, and 88.6% on using the Al_2O_3, Ni, and Al_2O_3–Ni-water nanofluid compared with water-fluid-operated FPC system. Likewise, the exergy is saved by 18.65, 51.49, and 70.89% on the adaptations of Al_2O_3, Ni, and Al_2O_3–Ni-water nanofluid compared with water-fluid-operated FPC system. However, its operating environmental temperature (absorber temperature) enhanced by the implementations of nanofluid is proven.

Table 5 Comparison of previous PTC receiver with the current system

References	Findings	Efficiency/%
Tong et al. [20]	Incorporating 1 vol% Al_2O_3/water nanofluid FPC	56.9
Azim et al. [25]	Utilizing $NiFe_2O_4$/water nanofluid in FPC at 0.050 kgs^{-1} flow rate	44.96
Present work	The Al_2O_3–Ni nanofluid FPC at 0.068 kgs^{-1} flow rate	72.8

Table 6 Details of energy saving and its environmental conditions

Descriptions	Water	Al_2O_3 nanofluid	Ni nanofluid	Al_2O_3–Ni–water nanofluid
Thermal efficiency	38.6	51.7	66.9	72.8
Exergy efficiency	13.4	15.9	20.3	22.9
Thermal energy savings	0	33.9	73.31	88.6
Exergy energy savings	0	18.65	51.49	70.89
Operating environment temperature rise in °C	28–35	28–55	28–50	28–77

Conclusions

This study examines the thermal performance of FPC for HVAC applications using different flow rates and various working fluids. The experiments were conducted with water and nanofluids, including Al_2O_3, Ni, and Al_2O_3–Ni, at different flow rate conditions, such as 0.028, 0.041, 0.055, and 0.068 kgs^{-1}. Incorporating nanofluids within the FPC system substantially improved the thermal behavior of the current research fluid medium, resulting in superior thermal performance compared to using water alone. This study has led to the following conclusions:

- With the significance of hybrid nanofluid, the FPC adopted with Al_2O_3/Ni/water hybrid nanofluid functioned by 0.068 kgs^{-1}flow rate and recorded better thermal performance than other combinations. Its thermal and exergy efficiency is enhanced by 72.8 and 22.9%, respectively, and compared to the thermal and exergy efficiency of water-functioned FPC, it is limited by 51.7 and 13.4%, respectively.
- Furthermore, the heat transfer coefficient and Nusselt number exhibited 58.3% and 52.6% higher, respectively, when using Al_2O_3–Ni nanofluid related to the fluid medium of water at the higher flow rate.
- The entropy of the present system shows a downtrend, while 1.2 WK^{-1} spots increased flow rate and optimum entropy generation on a hybrid nanofluid.
- Likewise, the COP of a hybrid nanofluid-operated FPC system was enhanced by 29.5% compared to the conventional system.

Incorporating nanoparticles into water significantly improved heat transfer characteristics and played a crucial role in determining FPC efficiency. Notably, Al_2O_3–Ni/water nanofluid demonstrated the maximum energy and thermal efficiency related to other kinds of fluid mediums under a high flow rate.

Acknowledgements The authors would like to acknowledge the Researchers Supporting Project number (RSP2024R373), King Saud University, Riyadh, Saudi Arabia.

Author contributions All authors contributed to the study's conception and design. The first draft of the manuscript was written by RV, and the individual contributions of ALL authors are given below: LS was involved in formal analysis, MA helped with methodology and writing, IH, SP, and AHS helped with investigation, KM participated in review and editing, VM and MAK helped with writing and language help, and RV participated in original draft preparation, supervision, and validation. All authors read and approved the final manuscript.

Funding The authors did not receive support from any organization for the submitted work.

Data availability All the data required are available within the manuscript.

Declarations

Conflict of interest The authors have no competing interests to declare relevant to this article's content.

Ethics approval This is an observational study. Influences of alumina, nickel, and alumina/nickel oxide nanofluid on thermal behavior of solar collector; Research Ethics Committee has confirmed that no ethical approval is required.

References

1. Oloruntobi O, Mokhtar K, Mohd Rozar N, Gohari A, Asif S, Fatt CL. Effective technologies and practices for reducing pollution in warehouses - a review. Cleaner Eng Technol. 2023;13: 100622. https://doi.org/10.1016/j.clet.2023.100622.
2. Gao D, Hao Y, Pei G. Investigation of a novel space heating scheme based on evacuated flat-plate solar collector and virtual energy storage. Appl Therm Eng. 2023;219: 119672. https://doi.org/10.1016/j.applthermaleng.2022.119672.
3. Li X, Zeng G, Lei X. The stability, optical properties and solar-thermal conversion performance of SiC-MWCNTs hybrid nanofluids for the direct absorption solar collector (DASC) application. Sol Energy Mater Sol Cells. 2020;206: 110323. https://doi.org/10.1016/j.solmat.2019.110323.
4. Syam Sundar L, et al. Efficiency analysis of thermosyphon solar flat plate collector with low mass concentrations of ND–Co_3O_4 hybrid nanofluids: an experimental study. J Therm Anal Calorim. 2021;143:959–72. https://doi.org/10.1007/s10973-020-10176-1.
5. Rangabashiam D, Ramachandran S, Sekar M. Effect of Al_2O_3 and MgOnanofluids in heat pipe solar collector for improved efficiency. Appl Nanosci. 2023;13:595–604. https://doi.org/10.1007/s13204-021-01865-w.
6. Salman AM, Anead HS, Sultan KF. An experimental investigation on the effect of hybrid Nanofluid (Al+ Al_2O_3/distilled water) on the thermal efficiency of evacuated tube solar collector. IOP Conf Series Mater Sci Eng. 2020;745:1. https://doi.org/10.1088/1757-899X/745/1/012073.
7. Dehaj MS, Rezaeian M, Mousavi D, Shamsi S, Salarmofrad M. Efficiency of the parabolic through solar collector using $NiFe_2O_4$/Water nanofluid and U-tube. J Taiwan Inst Chem Eng. 2021;120:136–49. https://doi.org/10.1016/j.jtice.2021.02.029.
8. Khanlari A. The Effect of utilizing Al_2O_3-SiO_2/deionized water hybrid nanofluid in a tube-type heat exchanger. Heat Transfer Res. 2020;52:991–1005. https://doi.org/10.1615/HeatTransRes.2020034103.
9. Elshazly E, Rehim AAA, Mahallawi IE. 4E study of experimental thermal performance enhancement of flat plate solar collectors using MWCNT, Al_2O_3, and hybrid MWCNT/ Al_2O_3 nanofluids. Res Eng. 2020;16: 100723. https://doi.org/10.1016/j.rineng.2022.100723.
10. Kaya H, Alkasem M, Arslan K. Effect of nanoparticle shape of Al_2O_3/Pure Water nanofluid on evacuated U-Tube solar collector efficiency. Renew Energy. 2020;162:267–84. https://doi.org/10.1016/j.renene.2020.08.039.
11. Bayram K, Osman I. Thermodynamic analysis of absorption cooling system with LiBr-Al_2O_3/water nanofluid using solar energy.

Therm Sci. 2022;26:135–46. https://doi.org/10.2298/TSCI200817340K.
12. Ukueje WE, Abam FI, Obi A. A perspective review on thermal conductivity of hybrid nanofluids and their application in automobile radiator cooling. J Nanotechnol. 2022. https://doi.org/10.1155/2022/2187932.
13. Kumar PG, Prabakaran R, Sakthivadivel D. Ultrasonication time optimization for multi-walled carbon nanotube based Therminol-55 nanofluid: an experimental investigation. J Therm Anal Calorim. 2022;147:10329–36. https://doi.org/10.1007/s10973-022-11298-4.
14. ASHRAE (2003) Standard, Methods of Testing to Determine the Thermal Performance of Solar Collectors. 3rded.Atlanta: GA, USA
15. Selimefendigil F, Irin CS, Oztop HF. Experimental analysis of combined utilization of CuO nanoparticles in latent heat storage unit and absorber coating in a single-slope solar desalination system. Sol Energy. 2022;233:278–86. https://doi.org/10.1016/j.solener.2022.01.039.
16. Sharafeldin MA, Grof G, Nada EA, Mahian O. Evacuated tube solar collector performance using copper nanofluid: energy and environmental analysis. Appl Therm Eng. 2019;162: 114205. https://doi.org/10.1016/j.applthermaleng.2019.114205.
17. Coccia G, Nicola GD, Sotte M. Design, manufacture, and test of a prototype for a parabolic trough collector for industrial process heat. Renew Energy. 2015;74:727–36. https://doi.org/10.1016/j.renene.2014.08.077.
18. Mubarrat M, Mashfy MM, Farhan T, Ehsan MM. Research advancement and potential prospects of thermal energy storage in concentrated solar power application. Int J Thermofluids. 2023;20: 100431. https://doi.org/10.1016/j.ijft.2023.100431.
19. Henein SM, Rehim AAA. The performance response of a heat pipe evacuated tube solar collector using MgO/MWCNT hybrid nanofluid as a working fluid. Case Stud Therm Eng. 2022;33: 101957. https://doi.org/10.1016/j.csite.2022.101957.
20. Tong Y, Lee H, Kang W, Cho H. Energy and exergy comparison of a flat-plate solar collector using water, Al_2O_3nanofluid, and CuOnanofluid. App Ther Eng. 2019;159: 113959. https://doi.org/10.1016/j.applthermaleng.2019.113959.
21. Malika M, Sonawane SS. The sono-photocatalytic performance of a Fe_2O_3 coated TiO_2 based hybrid nanofluid under visible light via RSM. Colloids Surf a Physico chem Eng Asp. 2022. https://doi.org/10.1016/j.colsurfa.2022.128545.
22. Ekiciler R, Arslan K, Turgut O. Application of nanofluid flow in entropy generation and thermal performance analysis of parabolic trough solar collector: experimental and numerical study. J Therm Anal Calorim. 2023;148:7299–318. https://doi.org/10.1007/s10973-023-12187-0.
23. Lattieff FA, Mahdi MA, Majdi JM, Talebizadehsardari P, Yaïci W. Performance analysis of a solar cooling system with equal and unequal adsorption/desorption operating time. Energies. 2021;14:6749. https://doi.org/10.3390/en14206749.
24. Smaisim, Fadhil G, Hussein A, Abdullah W, Abed, Azher M. Enhancement of heat transfer from solar thermal collector using nanofluid. Open Eng. 2022;12:968–76. https://doi.org/10.1515/eng-2022-0337.
25. Tuncer AD, Aytaç I, Variyenli HI, Khanlari A, Mantıc S, Karart A. Improving the performance of a heat pipe evacuated solar water collector using a magnetic NiFe2O4/water nanofluid. Ther Sci Eng Pro. 2023;45:102107. https://doi.org/10.1016/j.tsep.2023.102107.
26. Fedele L, Colla L, Bobbo S, Barsion S, Agresti F. Experimental stability analysis of different water based nanofluids. Nanoscale Res Lett. 2011;6:300. https://doi.org/10.1186/1556-276X-6-300.